

Mail hard copies to:
 Dr. Sixto González, Director
 Arecibo Observatory
 HC 3 Box 53995
 Arecibo, PR 00612 U.S.A.

ARECIBO OBSERVATORY
 NATIONAL ASTRONOMY AND
 IONOSPHERE CENTER
 OBSERVING TIME REQUEST
 COVER SHEET

We are indebted to our
 user community for their
 continued support of
 the Arecibo Observatory,
 Puerto Rico.

Section I - General Information

Submitted for Jun 1 2005.

This proposal has not been submitted before.

Proposal Type: Large
 General Category: Astronomy
 Sub-Category: Continuum
 Observation Category: Extragalactic
 Total Time Requested: 1512 Hours

Proposal Title: The G-ALFA Continuum Transit Survey

ABSTRACT:

As part of the GALFA consortium we propose to use Arecibo and ALFA to carry out a sensitive, high resolution, spectro-polarimetric survey of the Arecibo sky – the GALFA Continuum Transit Survey, GALFACTS. GALFACTS will be a major observational advance in imaging of the polarized radiation from the Milky Way and other galaxies, and promises a transformational advance in our understanding of the magnetic field of the Milky Way, the properties of the magneto-ionic medium, and the role of magnetic fields in galactic processes. We will also explore the polarisation properties of a vast number of extragalactic radio sources down to sub-mJy levels. GALFACTS will be a scientific pathfinder to the Square Kilometre Array in the area of cosmic magnetism, and will not be surpassed until the SKA turns on as survey instrument late in the next decade.

Name	Institution	E-mail	Phone	Student
Andrew R Taylor	University of Calgary	russ@ras.ucalgary.ca	1-403-220-6633	no
Christopher J Salter	NAIC/Arecibo Observatory	csalter@naic.edu	787-878-2612 x281	no

Additional Authors

Christy Bredeson,
 University of Calgary
 cbredeson@ras.ucalgary.ca

Chris Brunt
 University of Massachusetts
 brunt@fcrao1.astro.umass.edu

Mike Davis
 SETI Institute
 mdavis@seti.org

Jo-Anne Brown
 University of Calgary
 jocat@ras.ucalgary.ca

Avinash Deshpande
 NAIC/Raman Research Institute
 desh@naic.edu

Tyler Foster
 Dominion Radio Astrophysical
 Observatory

tyler.foster@nrc-cnrc.gc.ca

heiles@astron.berkeley.edu

Tom Landecker
Dominion Radio Astrophysical
Observatory
Tom.Landecker@nrc.gc.ca

Bryan Gaensler
Harvard-Smithsonian Center for
Astrophysics
bgaensler@cfa.harvard.edu

Han JinLin
Beijing Astronomical Observatory
hjl@ns.bao.ac.cn

Patrick Leahy
University of Manchester
jpl@jb.man.ac.uk

Tapasi Ghosh
NAIC
tghosh@naic.edu

Gilles Joncas
Universite Laval
joncas@phy.ulaval.ca

Emmanuel Momjian
NAIC
emomjian@naic.edu

Marijke Haverkorn
Harvard-Smithsonian Center for
Astrophysics
mhaverkorn@cfa.harvard.edu

Charles Kerton
Iowa State University
kerton@iastate.edu

Samar Safi-Harb
University of Manitoba
safiharb@cc.umanitoba.ca

Carl Heiles
University of California, Berkeley

Roland Kothes
DRAO/University of Calgary
Roland.Kothes@nrc.gc.ca

I will not need financial support.

This work is part of both a PhD and a MS thesis.

Service Observing Request

Remote Observing Request

- None
- All of the observing run.
- Part of the observing run.
- Queue Observing

- No
- Maybe
- Yes

Section II - Time Request

The following times are in LST.

Begin – End Interval–Interval	Days Needed at This Interval
o – 24	28
0 – 24	28
0 – 24	7
–	

Time Constraints (Must Be Justified in the Proposal Text)

observations must be carried out at night time

As detailed in the proposal we request one session every three months for four years. Each session consisting of 28 nights with 3 hours per night covering the same 3 hour LST range.

In year 5 we require four sessions each of 6 hours per night for 7 nights.

Section III - Instruments Needed

ALFA

Atmospheric Observation Instruments:

Special Equipment or setup: P-ALFA/GALFA Continuum spectrometer

Section IV - RFI Considerations

Frequency Ranges Planned

1225 - 1525

This proposal requires coordination with Punta Salinas radar within the band 1222-1381 MHz..

This proposal requires coordination with GPS L3 at 1381 MHz.

Section V - Observing List

Target List

GALFACTS: The G-ALFA Continuum Transit Survey

Christy Bredeson	University of Calgary
Jo-Anne Brown	University of Calgary
Chris Brunt	University of Massachusetts
Avinash Deshpande	NAIC/Raman Research Institute
Mike Davis	SETI Institute
Tyler Foster	Dominion Radio Astrophysical Observatory
Bryan Gaensler	Harvard-Smithsonian Center for Astrophysics
Tapasi Ghosh	NAIC
Marijke Haverkorn	Harvard-Smithsonian Center for Astrophysics
Carl Heiles	University of California, Berkeley
Han JinLin	Beijing Astronomical Observatory
Gilles Joncas	Université Laval
Charles Kerton	Iowa State University
Roland Kothes	DRAO/University of Calgary
Tom Landecker	Dominion Radio Astrophysical Observatory
Patrick Leahy	University of Manchester
Emmanuel Momjian	NAIC
Samar Safi-Harb	University of Manitoba
Chris Salter	NAIC
Russ Taylor (Principal Investigator)	University of Calgary

1 June 2005

1 Introduction

Arecibo is the world's largest single-dish radio telescope, achieving continuous spatial frequency coverage, high surface brightness sensitivity, and arcmin-scale resolution at decimetre wavelengths. The ALFA multi-beam receiver system allows these properties to be used to image large areas of the sky at $\lambda 21$ cm. As part of the GALFA consortium we propose to use Arecibo and ALFA to carry out a sensitive, high resolution, spectro-polarimetric survey of the Arecibo sky – the GALFA Continuum Transit Survey, GALFACTS.

A key objective of the ALFA continuum survey is images of the polarized emission from our Galaxy and a vast population of extragalactic sources. Wide-field polarimetric imaging has enjoyed a surge of activity over the past several years with the discovery of highly structure arcminute scale polarized radiation in interferometric images, both at high Galactic latitude in WSRT 349-MHz images (Haverkorn *et al.* 2003b), and in the Canadian Galactic Plane Survey (CGPS, Taylor *et al.* 2003) and Southern Galactic Plane Survey (SGPS, Gaensler *et al.* 2001) at 1.4 GHz. These structures are superposed on the polarized emission from SNRs and the diffuse Galactic synchrotron emission, but themselves have no Stokes-I counterpart. The accepted interpretation is that the distributed polarized emission arises from the intrinsically-smooth Galactic synchrotron emission, but differential Faraday rotation in the intervening magneto-ionic medium (the Faraday Screen) imposes fine structure on this; i.e. propagation effects dominate over intrinsic polarized structure. This emerging field is now moving from phenomenology to astrophysics, the signatures of the Faraday Effect on polarization revealing details of the interstellar magnetic field (RMs of compact sources) and of the magneto-ionic medium (imaging of extended emission).

GALFACTS will be a major observational advance in imaging of the polarized radiation from the Milky Way (and other galaxies) and promises a transformational advance in our understanding of the magnetic field of the Galaxy and the properties of the magneto-ionic medium. Presently, the highest resolution, single-dish, L-band continuum surveys are those of Reich *et al.* (1997) in the Galactic plane ($|b| \leq 4^\circ$), and Uyaniker *et al.* (1999) of a few selected regions at intermediate latitudes, both with resolution of $9.4'$ and brightness sensitivities of 10's of mK. For surveys covering a significant fraction of the sky, only significantly poorer resolution data are available ($\theta_{\text{HPBW}} = 35'$, Reich *et al.* (2001) and Wolleben *et al.* (2005)). In comparison, GALFACTS will provide full-Stokes image cubes at resolution of $3.3'$, brightness sensitivity over an order of magnitude higher than previous work, and cover a band of 1225 – 1525 MHz, in spectral-line mode, allowing imaging of Faraday Rotation Measure.

The images of the polarized sky by GALFACTS will not be superseded until the SKA turns on as a survey instrument late in the next decade. Understanding the origins and evolution of cosmic magnetism has been identified as one of the key science drivers for the SKA. GALFACTS will be a scientific pathfinder to the SKA in this area. GALFACTS will also provide us with our best knowledge of the polarized “foreground” sky; crucial information for the *Planck* space mission, to be launched in 2007/8 with the aim of mapping the polarized structure of the CMB on scales of a few arcminutes.

2 Science Objectives

2.1 The Galactic Magnetic Field

2.1.1 Global Structure of the Galactic Magnetic Field

Optical and radio polarization studies have established that the Milky Way and many other nearby spiral galaxies all show well-organized, large-scale magnetic fields Beck *et al.* (1996); Han & Wielebinski (2002). The presence of coherent magnetic fields on large scales points to a powerful and ubiquitous process which organizes random motions into highly-ordered structures. Galaxies and clusters are likely formed from collisions of smaller constituents, and then are continually energized by galaxy mergers, stellar winds and supernovae — it is thus remarkable that the magnetic fields produced by the resulting complicated gas flows and electrical currents are some of the largest organized structures in the Universe. The dynamo mechanism, in which small-scale turbulent magnetic fields are amplified and ordered by cyclonic motions and differential rotation, is the favoured explanation to account for this structure Beck *et al.* (1996). However, dynamos are not fully understood and still face theoretical problems.

For most external galaxies, polarized synchrotron emission provides useful information on the geometry of the magnetic field (see Section 2.1.2), but tells us little about the field's direction. Since dynamo models are characterized by field *coherence*, Faraday rotation is needed to provide the extra information needed to understand dynamos and the fields that they generate. Our own Milky Way is an excellent test-bed to address these issues, because it covers a sufficiently large solid angle that a huge ensemble of background extragalactic RMs can be used to probe the three-dimensional magnetic field structure. Indeed, RMs for pulsars and for extragalactic sources have allowed us to identify reversals in the spiral magnetic pattern of our Galaxy (Brown & Taylor 2001; Han *et al.* 2002) and to measure the polarity of the vertical structure of the Galaxy's magnetic field (e.g., Han *et al.* 1997), both of which are key to understanding the dynamo process. Unfortunately, the sparse sampling of RMs over most of the sky (see Fig. 1) makes it difficult to establish any consensus on these issues.

Using the differential source count distribution in polarization predicted by Beck & Gaensler (2004), we predict that GALFACTS will yield RMs for $\sim 30,000 - 40,000$ polarized background sources, spread in a continuous distribution over all Galactic latitudes, and covering both the inner and outer Galaxy. Given that there are currently only ~ 1600 background RMs known over the entire sky, $\sim 50\%$ of which are concentrated into into relatively small regions corresponding to the CGPS and SGPS, (see Fig. 1), it is clear that GALFACTS will bring us into an entire new regime for studying foreground magnetic behaviour. Below we outline some of the topics that we will explore with this data-set.

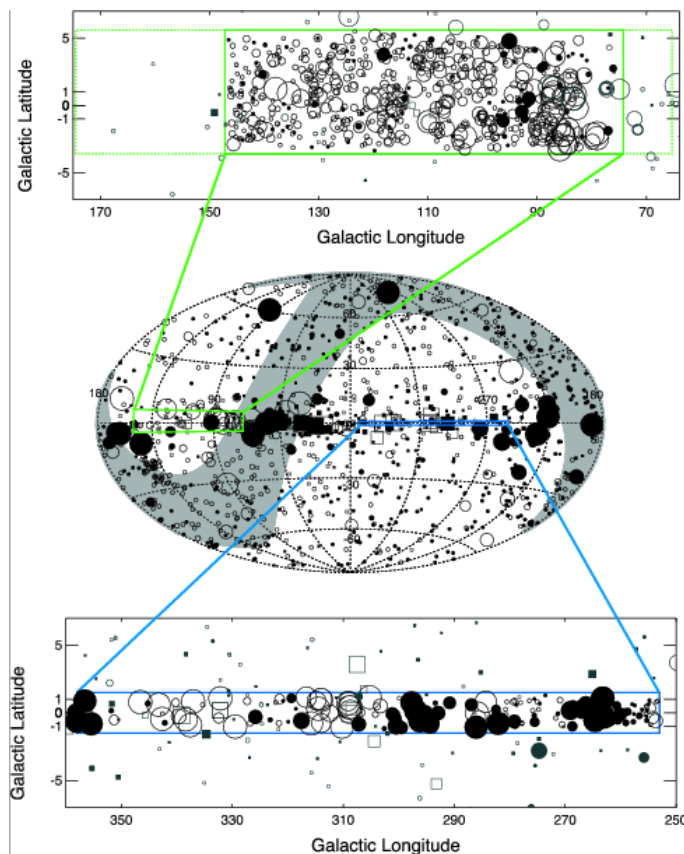


Figure 1: Current status of point-source RM measurements over the entire sky. The central panel is an Aitoff projection of the sky in Galactic coordinates, showing the 887 extragalactic RMs and 316 pulsar RMs that were known before the advent of the CGPS and SGPS. The top panel highlights the 600 new extragalactic RM sources in the CGPS region; the bottom panel shows the 151 new RM sources in the SGPS region. Closed symbols represent positive RMs, and open symbols negative RMs; extragalactic sources are shown as circles while pulsars are marked as squares. In the range $100 < |\text{RM}| < 600 \text{ rad m}^{-2}$, the size of the symbol is proportional to $|\text{RM}|$; for magnitudes of RM outside this range, the sizes of symbols are fixed. The shaded region indicates the sky coverage of the GALFACTS survey. GALFACTS will increase the total number of RMs by more than an order of magnitude, covering almost the entire range of Galactic latitude, and longitudes in the inner and outer Galactic plane that are complementary to the interferometric surveys.

Halo and Disk-Halo Interaction

Possibly the most significant contribution offered by GALFACTS is the possibility of looking at magnetic fields in the halo. While there have been several studies targeting the large-scale field in the disk (e.g. Rand & Lyne, 1994; Indrani & Deshpande, 1998; Brown & Taylor, 2001), there have been very limited studies of the halo field Han & Qiao (1994), and even less of the disk-halo interface Beck (2001). While we know that a magnetic field exists in the halo, and that it is significantly weaker than in the disk, definitive statements regarding the nature of the halo field are impossible because of the paucity of RM data available in this region. The numerous plumb-lines provided through the halo by GALFACTS will reveal the geometry and symmetry of the halo field, providing a discriminant on which dynamo mode(s) are operating in the Galaxy, and possibly indicating if a different dynamo operates in the halo compared to the disk. Furthermore, the structure of the transition between the halo field and the disk field is completely unknown. In this interface region of exchange of mass and energy, magnetic fields are likely to play an important role. The unique sky coverage of GALFACTS is ideal for probing this region.

Large-scale field symmetry in the Disk

The topologies of magnetic fields in galactic disks are broadly classified into axisymmetric (ASS), bisymmetric (BSS), and mixed (MSS) spiral structure. The distinguishing symmetry axis between ASS

and BSS galaxies is with respect to a π rotation of the disk. In the case of ASS galaxies the geometry of the field is the same with respect to this axis, whereas in BSS galaxies the field direction reverses with a π rotation of the disk. Galaxies observed to have a combination of ASS and BSS structure are classified as MSS. Different mechanisms of field generation and maintenance will lead to different symmetries. For example, the lowest-order dynamo mode yields an ASS structure, while the first excited-mode produces a BSS structure. Characterizing these symmetries is of fundamental importance to our understanding of how galactic fields are generated and maintained.

The type of observations presently available allow us to identify some qualitative features of large-scale galactic fields. One such important feature are magnetic field reversals, corresponding to regions of shear across which the field abruptly changes sign. Recent work from the IGPS (Brown et al. 2005, in prep.), suggests a strong correlation of the disk field with the spiral arms, and there is evidence to suggest that there may only be one significant field reversal inside the solar circle. As shown in Figure 1, there is a sharp transition in the sign (and magnitude) of RMs in the Galactic plane at $l \sim 300^\circ$, and there is tentative evidence that a similar transition occurs at $l \sim 60^\circ$. However, the sampling of background RMs in the Galactic first quadrant is extremely limited. By providing Galactic longitude coverage that is complementary to the CGPS and SGPS, and covers the crucial first quadrant, GALFACTS will yield the data to test this prediction. The presence or absence of such a reversal can provide a crucial constraint in determining the field geometry in the disk, and consequently can establish which dynamo modes operate in our own Milky Way.

2.1.2 Magnetic Fields in Nearby Galaxies

Magnetic fields play a major role in the interstellar medium, and make a significant contribution toward balancing the ISM against gravitation (Beck 2004). Thus, understanding magnetic fields in galaxies is of crucial importance for understanding their formation and evolution.

In spiral galaxies, the configuration of magnetic fields is intimately related to the magnetohydrodynamic behaviour of interstellar gases, and is closely linked to the formation of gaseous arms and magneto-ionic halos surrounding the galactic disks (Sofue *et al.* 1986). Previous linear polarization mapping of nearby spiral galaxies, as well as various statistical data, have suggested that magnetic fields and star formation activity in spiral arms are closely correlated (Sofue *et al.* 1986, Beck *et al.* 1996). However, there are indications of deviations from the large-scale structures both in the spiral arms and in the centres of galaxies. In several cases, regular fields are concentrated between the optical spiral arms.

As linearly polarized radio continuum emission is a powerful tool to study the strength and structure of interstellar magnetic fields in galaxies, the GALFACTS survey would make it possible to carry out full Stokes mapping of large ($> 10'$), nearby (mostly spiral) galaxies, adding significant information on the structures and magnetic field configurations within these objects. There are 17 galaxies with angular size greater than $10'$ in the GALFACTS area and over 50 larger than $7'$. The positional variation of the rotation measure over a galaxy could be used to study the configuration of a global magnetic field under the assumption that the field is distributed in the plane of the galaxy. This allows to distinguish between the two predominant configuration of the large scale field in a spiral galaxy, which is either bisymmetric, with the lines of force possibly open to intergalactic space, or a ring with closed circular field lines in the disk (Sofue et al. 1986).

2.2 The Magneto-Ionic Medium

2.2.1 Understanding the Faraday Screen

The presence of an ordered component to the ISM's overall magnetic field is implied by the diffuse polarized radio emission seen throughout the Milky Way. This emission has been successfully modelled as a superposition of thin and thick disks of magneto-ionic material, both of which exhibit spiral structure (Beuermann *et al.* 1985). As mentioned previously, images of polarization intensity, position

angle reveal intricate polarized structures such as filaments, canals and rings over a wide range of angular scales. These features imply a complicated mixture of synchrotron emission and Faraday rotation (e.g., Gaensler *et al.*, 2001; Uyaniker *et al.*, 2003). Other features are artifacts of differential Faraday rotation (“Faraday ghosts”) and may give us new information about the properties of the turbulent interstellar medium (Shukurov & Berkhuijsen 200). To distinguish and interpret these phenomena, new approaches have to be developed.

A fundamental limitation of previous studies is that just a single RM value per image pixel has been derived, while in fact we expect extended polarized emission to be well spread in depth along a given line of sight. Thus, for each image pixel, different polarized structures at different depths have distinct foreground Faraday rotation signatures. We can separate out these structures through “RM tomography”, in which for each pixel we Fourier transform Faraday-induced modulations in Stokes Q and U as a function of frequency into a spectrum of linearly polarized intensity as a function of “Faraday depth” (Ramkumar & Deshpande, 1999; Brentjens & de Bruyn, 2004, see). In this way, Rotation Measure data cubes (analogous to spectral-line cubes) can be formed with the axes (l , b , RM).¹ This approach allows us to carry out a unique three-dimensional dissection of interstellar magnetism, which will reveal the shells, filaments and sheets in which ordered magnetic fields are distributed throughout the Galaxy. ALFA offers attractive possibilities for such studies. With its 300 MHz bandwidth, and about 1000 channels, it should be possible to probe the entire range of physically expected RMs with an RM resolution of $\sim 150 \text{ rad m}^{-2}$ (RMs of individual features will be determined to far better accuracy).

While RM tomography is now being tried by other groups, their telescopes are limited by poor precision in RM and the restricted spatial sensitivity of interferometric studies. The broad bandwidth single-dish study offered by GALFACTS will not share these shortcomings, producing a view of the overall structure of interstellar magnetic fields and of diffuse polarized emission throughout the Galaxy that will be an order of magnitude more sensitive, more accurate and more revealing than all other efforts.

2.2.2 Magnetic Fields and Star Formation

An outstanding and largely unexplored question is the role of magnetic fields in the cold neutral medium. Magnetic fields are thought to be an important factor in the formation of molecular clouds and in generating the conditions for star formation (Heiles 1993), but observational data to impact theory are sparse. Polarimetry of dust emission at submm wavelengths (e.g., Matthews, Fiege and Moriarty-Schieven 2002) has been carried out on a few clouds. Such data provide information on the direction of the magnetic field projected onto the plane of the sky but no information on the magnetic field strength. A new avenue to explore magnetic fields in the cold neutral medium is promised by recent CGPS results that show polarization position angle variations on the synchrotron background due to dust clouds (see Fig. 2). This structure in position angle is imposed by the differential Faraday rotation as the synchrotron radiation propagates through the cloud. Polarimetry from *Herschel*, and models of the ionization within the cloud, can provide a new window on the both the magnitude and orientation of the magnetic fields within dust clouds. The GALFACTS survey will provide sensitive polarization maps covering the extents of several nearby molecular clouds, providing a unique way to study structure at the magnetic field structure in the molecular ISM, as well as the interface between a molecular cloud and the ambient medium (see section 2.2.3).

2.2.3 Magnetic Fields in Individual Objects

HII Regions and Molecular Clouds

HII regions provide a link between the molecular clouds from which stars form, the powerful winds which massive stars generate, and the ambient interstellar medium (ISM) into which all this material

¹The usual Fourier inverse relationships apply between (a) the spectral resolution and the measurable RM range, and (b) the full spectral bandwidth and the RM resolution.

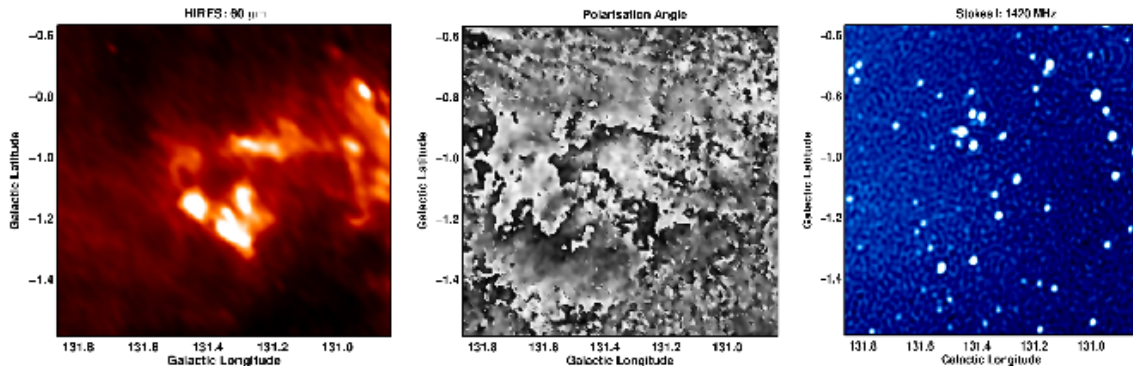


Figure 2: Faraday rotation of the background synchrotron radiation as a result of propagation through a dust cloud. The left images shows an IRAS image of 60 micron emission from a complex of dust clouds. The central image is the polarization position angle from the same image. The cloud is seen to impose structure on the position angle map due to differential Faraday rotation. The 1420 MHz continuum image at right shows there is no HII region associated with the dust.

ultimately diffuses. Because HII regions span a very wide range of densities, studies of magnetic fields in HII regions provide an insight into how magnetic fields control the flow of gas, and conversely how compression of gas can amplify magnetic fields (Troland & Heiles 1986). Zeeman splitting of masers can probe magnetic fields in ultra-compact HII regions, but it is difficult to measure magnetic fields in more diffuse sources.

Polarization data from GALFACTS will provide a wealth of information on magnetic fields and Faraday rotation in these objects. In particular, since HII regions are Faraday active, they can *depolarize* the diffuse background radiation, allowing us to determine the physical conditions within their interiors. The underlying principle is that at a given observing wavelength and angular resolution, there is a direct relationship between the degree of depolarization observed and the magneto-ionic properties of the source (i.e. its electron density, magnetic field strength, and scale for turbulent fluctuations) Tribble (1991); Sokoloff *et al.* (1998). One can estimate n_e through observations in other wavebands, and then use polarization observations at two well-separated wavelengths to break the degeneracy between the other two magneto-ionic parameters.

An example is shown in Figure 3, where we show linear polarization in a region surrounding the HII region RCW 94. While there is bright linearly polarized background emission in other regions of the field, reduced polarization is seen interior to the source. Gaensler *et al.* (2001) show that this is due to beam depolarization, resulting from random variations in n_e and B within the source on small scales, which cause the polarization within a resolution element to average to zero. In combination with radio continuum and $H\alpha$ data, the degree of beam depolarization can be used to infer for RCW 94 an electron density $n_e \approx 20 \text{ cm}^{-3}$, a magnetic field strength $B \approx 2 \mu\text{G}$, and an outer scale for turbulent fluctuations $l_0 \approx 0.15 \text{ pc}$. This approach is a vast improvement over previous attempts at making such measurements — determinations of magnetic fields in the interiors of HII regions have relied on measuring an excess in the RMs of background sources and thus only result in upper limits Heiles *et al.* (1981), while to measure the scale of turbulence in such sources has previously required tens of thousands of optical spectra per object (Miville-Deschêne *et al.* 1995).

GALFACTS will be a rich resource for extending this technique. In conjunction with Arecibo HI surveys and (in regions of low extinction) $H\alpha$ data from recently released all-sky surveys (Dennison *et al.* 1999; Gaustad *et al.* 2001), this will allow us to determine the properties of every HII region whose presence can be seen against the polarized background. The fact that GALFACTS covers such a large part of the sky allows us to build up a statistically useful sample on these objects. With these data, we can correspondingly begin to characterize how gas and magnetic fields are compressed by ionization fronts, how the ionization fraction within photo-dissociation regions varies with distance from the central star, and what role magnetism plays in the highly turbulent interiors of HII regions.

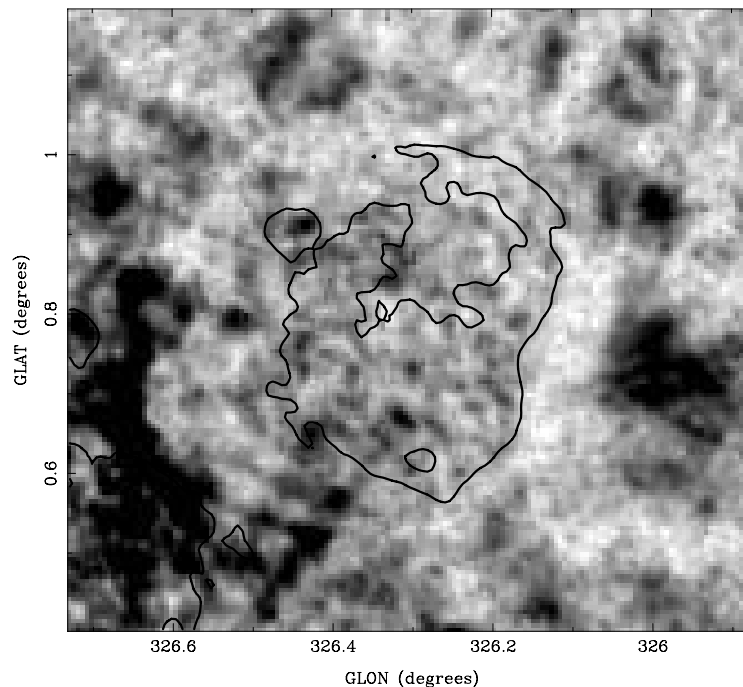


Figure 3: Linear polarization towards the HII region RCW 94, as observed in the Southern Galactic Plane Survey (Gaensler *et al.* 2001). The greyscale represents linearly polarized intensity at 20 cm, while the contour corresponds to the boundary of the source as seen in radio continuum emission. Reduced polarization can be seen towards the interior of RCW 94, while a halo of complete depolarization encloses the source's perimeter.

Furthermore, we note that foreground depolarization can be used to study the photo-dissociation regions produced by the interaction between stars and their nascent molecular clouds. Returning to Figure 3, it can be seen that as well as reduced polarization in the interior of RCW 94, there is also a halo of complete depolarization in an annulus around its perimeter. Gaensler *et al.* (2001) have shown that this must be due to a sharp *gradient* in RM around the source, suggesting that RCW 94 is embedded in a low density cocoon. By comparing these data to CO and HI observations, we demonstrated that RCW 94 is interacting with a molecular cloud and that this low density cocoon corresponds to partially ionized material resulting from the shock driven into the cloud by the HII region. Polarization data thus allow us to directly probe this interaction (see also Wolleben & Reich, 2004).

Finally, we note that polarization observations have revealed unusual structures which have no counterpart in total intensity or at any other wavelength (Fig. 4; Gray *et al.*, 1998; Uyaniker & Landecker, 2002; Haverkorn *et al.*, 2003b). It is currently unclear whether these features are magnetic funnels, flux tubes, old supernova remnants, or some other, new, phenomenon. In the 12 700 square degrees of the GALFACTS survey, there will assuredly be further examples of such sources, the properties of one of which or of the combination might provide clues as to their nature. The broad bandwidth coverage of the GALFACTS observations will also allow detailed RM tomography studies of these objects (see Section 2.2.1), which can allow us to better establish these sources' magneto-ionic properties and overall geometry.

Supernova Remnants

Magnetic fields in SNRs are a key diagnostic of the physical processes which govern heating, turbulence and particle acceleration generated by strong shocks. Magnetic field strengths in SNR shocks are typically thought to be at the level of $\lesssim 1\text{mG}$ (Fürst & Reich 2004), but it is unclear how these high magnetic fields are produced, especially in young adiabatic SNRs where the compression ratio is small. Turbulent amplification in Rayleigh-Taylor unstable regions between the forward and reverse shocks of the SNR can generate strong magnetic fields (Jun & Norman 1996a,b). This may in turn result in

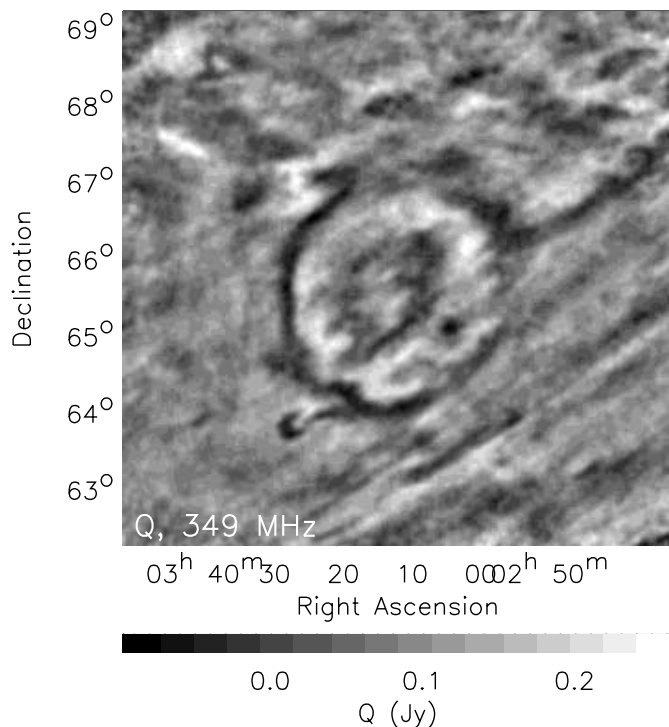


Figure 4: A “magnetic tunnel”, seen only in polarization, as imaged by WSRT at 349 MHz (Haverkorn *et al.* 2003b). The greyscale shows Stokes Q from this source; it is not seen in total intensity or at any other wavelength.

significant second-order Fermi acceleration of cosmic rays, and could have an important bearing on the overall evolution of SNRs (Ostrowski 1999; Gaensler & Wallace 2003).

With current data we are unable to address these issues. While the position angle of polarized emission provides the *orientation* of the magnetic field (Milne 1990; Fürst & Reich 2004), we normally do not have a good estimate of the field *strength* in these regions, because there is little reason to assume that magnetic fields and cosmic rays are in equipartition. Only in a few sources can we directly infer the magnetic field strength via Zeeman splitting of shock-excited OH masers (Brogan *et al.* 2004), but these are likely to be special cases where the shock is radiative and is interacting with a molecular cloud (Chevalier 1999). GALFACTS offers a major step forward in our understanding, in that the diffuse polarized background which we will detect at high signal-to-noise will allow us to directly measure magnetic fields in these sources. Specifically, we will combine the enhancements in RM seen against SNRs with observations of thermal X-rays from SNR shocks to separate out density and magnetic field contributions to the RM (Matsui *et al.* 1984). In the survey field covered by GALFACTS, this technique can be applied to many SNRs, embedded in many different environments, and at a wide range of evolutionary stages.

It is widely believed that supernova remnants (SNRs) accelerate cosmic rays through diffusive shock acceleration. An important part of this process is that particles streaming away from the shock generate enhanced magnetohydrodynamic turbulence just upstream, which in turn provides the scattering centres which reflect particles back across the shock (e.g., Achterberg *et al.* , 1994). Because of this process, it is reasonable to suppose that SNR shocks inject significant amounts of turbulent energy into their surroundings, which ultimately become part of the overall turbulent cascade. These physical processes can be directly tested by observations of RMs of background sources, in that we expect to see enhanced amplitudes and dispersions of RMs immediately beyond the bright radio rims of young SNRs. A preliminary effort in this regard tentatively suggests that indeed there is a larger scatter in the RMs of sources behind SNRs than in other regions (Simonetti 1992), but from the crude statistics of that study it is difficult to make definitive statements.

Many of the SNRs that will be covered by the GALFACTS survey will be nearby and hence of large angular diameter ($> 1 \text{ deg}^2$). In addition, GALFACTS will likely identify several new SNRs, too large and too faint to have been previously identified. For each of these SNRs and their immediate surroundings, GALFACTS will provide both diffuse and discrete RM measurements, which can trace the enhanced fluctuations produced by shock acceleration. This dense sampling of RM, accumulated over many SNRs, can provide a definitive study of turbulence in SNR shocks.

2.2.4 Turbulence in the Magneto-ionic Medium

In the past decades the paradigm describing the ISM has been slowly shifting from an equilibrated, more-or-less static medium consisting of “clouds” to a continually evolving, turbulent gas at a broad range of temperatures, densities and ionization states (e.g. Ferrière 2001). Interstellar turbulence plays a critical role in a variety of physical processes including star formation, cosmic ray propagation and the energy balance of the gas (e.g. Elmegreen & Scalo 2004). But due to the complexity of the gas and the variety of physical processes involved, theory is necessarily heavily oversimplified and observations give widely varying results depending on frequency, line of sight and method (e.g. Armstrong *et al.* 1995, Minter & Spangler 1996, Haverkorn *et al.* 2003). Therefore, fundamental questions regarding the physical characteristics of the ISM turbulence and its driving sources remain unanswered.

Rotation measure fluctuations can be quantitatively analyzed using structure functions, equivalent to power spectrum analysis. This method has proved to be a fruitful way to characterize the structure in RM. Usually the structure function is described by a power law. Saturation of the power law indicates a typical scale of energy injection, whereas the slope of the structure function gives information on the kind of fluctuations or turbulence in the medium. Furthermore, directional differences in one-dimensional structure functions can be used to study anisotropies in the RM distribution (Haverkorn *et al.* 2004). This statistical analysis of GALFACTS polarimetric data will allow us to explore several aspects of turbulence in the ISM.

First, applying RM tomography to the GALFACTS RM maps will allow us to characterize the magneto-ionic fluctuations of the ISM as a function of position and environment throughout the Galaxy. Typical scales of energy injection in the medium are seen to differ with Galactic environment (Haverkorn *et al.* 2004, 2005). The GALFACTS survey will allow the study of sources of ISM fluctuations as a function of Galactic longitude and latitude, enabling us to distinguish between turbulence in spiral arms and interarm regions, and in the Galactic disk and halo.

Secondly, heating by dissipation of turbulence is theoretically expected to contribute significantly to the energy budget of the diffuse ISM (Minter & Spangler 1997). Indeed, the observed properties of the ISM cannot be modelled with photo-ionization heating alone, and inclusion of turbulence dissipation is necessary to reconcile observations with theory (Minter & Balser 1997). The large longitude and latitude range of the GALFACTS survey will allow studying the role of turbulent heating as a function of position, to explore its significance in the Galactic disk and halo.

Interstellar turbulence is highly anisotropic, as shown in observations of molecular clouds and interstellar scintillations on subparsec scales (Rickett & Coles 2005), as well as general theoretical considerations (Goldreich & Sridhar 1995, 1997). Statistical analysis of GALFACTS data can reveal this anisotropy in the ionized plasma, and explore its dependence on direction and environment.

Finally, very little is known about the presence of magneto-ionized turbulence in the Galactic halo, although characterizing the structure of the halo plasma and magnetic field is vital for Galactic dynamo models (e.g. Kulsrud 1999). High-latitude X-ray observations have revealed a pervasive hot gas in the Galactic halo which is described as having a ‘patchy structure’ (Ferrière 2001). Statistical analysis of the high-latitude data of the GALFACTS survey promises to give for the first time insight into the turbulent properties of the ionized gas in the Galactic halo on a range of scales.

2.3 Galactic Continuum Radiation

The full-Stokes capability of GALFACTS will lead to many advances in our understanding of the magneto-ionic medium in our Galaxy. For many of the project’s science goals the Stokes I images will tend to play a contextual or supporting role, for example in the identification of interesting Faraday depolarization structures without corresponding total intensity emission. However, the Stokes I images alone from the survey also represent a unique high-sensitivity and high spatial dynamic range (i.e. high resolution combined with wide spatial coverage) view of Galactic continuum emission that will form the basis of several interesting scientific investigations, a few of which are outlined in this subsection.

2.3.1 Low Surface Brightness Structures

We expect the combination of high sensitivity and arcminute-scale resolution will enable us to discover many new extended and low-surface brightness objects within the GALFACTS survey area. In particular we will investigate low surface brightness continuum emission associated with both the birth and death of high mass stars.

In the first case low surface brightness continuum emission can be associated with large HII regions both as a diffuse halo caused by ionizing photons “leaking” out of the main HII region, and with disk-halo structures such as chimneys (e.g., Normandeau *et al.* 1996; Terebey *et al.* 2003). Examination of the diffuse halo emission provides information on how porous HII regions are thus providing information on the source of ionizing photons for the diffuse warm ionized medium of our Galaxy. The spatial coverage of GALFACTS combined with its overlap with the Galactic plane will also allow us to investigate continuum emission associated with disk-halo structures. Knowledge of the ionized gas content and morphology associated with such structures can yield constraints on the evolution and energetics of such objects (e.g. Basu *et al.* 1999).

The second thrust of this project will be the identification of new supernova remnants (SNRs). In addition to detecting more diffuse evolved SNRs we also hope to detect younger SNRs that are evolving in a low density environment. A careful accounting of such objects is important as the vast majority of SNRs in our Galaxy should be those associated with the explosion of a massive progenitor star. In these cases the SNR will likely be expanding into a low density environment created by stellar winds associated with the star cluster of which they are a part. In such an environment a low surface brightness SNR is expected.

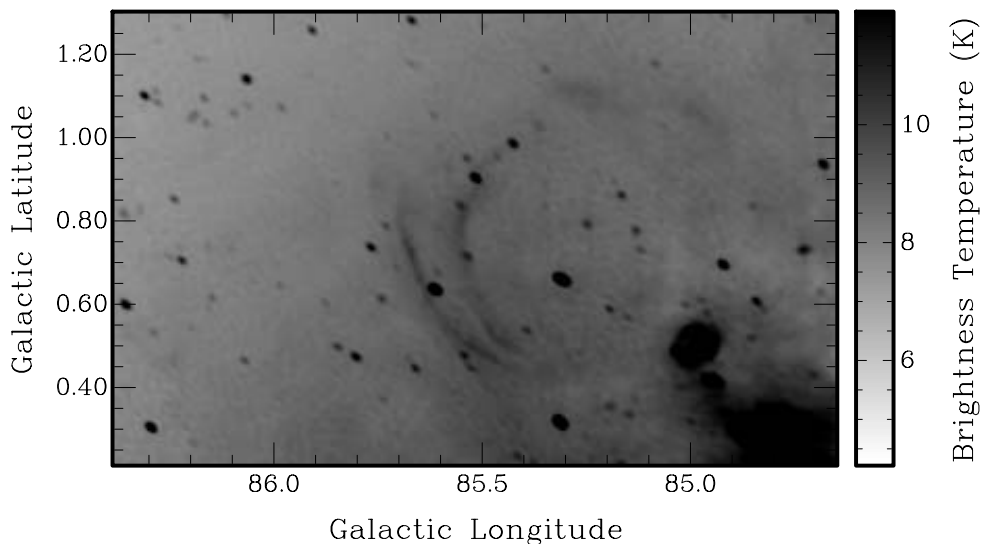


Figure 5: Two new low surface brightness supernova remnants G85.4+0.7 and G85.9-0.6 (Kothés *et al.* 2001). These new SNR discovered in the 1420 MHz continuum images of the CGPS Phase 1 survey illustrate how the combination of resolution and sensitivity are crucial in the detection such features

GALFACTS observations will complement the interferometric based searches of the Galactic plane by providing unique coverage of the Galactic plane in the third quadrant (i.e., in the gap between the CGPS and SGPS surveys) and extending the search to higher latitudes in other regions. The necessity for the combination of sensitivity and high spatial dynamic range is well illustrated by the newly discovered SNRs from the CGPS Phase 1 survey (Kothes *et al.* 2001).

The full Stokes data from GALFACTS will also be useful in the rapid identification of older, evolved SNR. For example Kothes (2003) recently identified the SNR G107.5-1.5 (see Figure. 5) in CGPS Phase-1 data on the basis of the strong polarized emission seen in the complementary polarization images. In this case the high percentage polarization of the object suggests that the SNR is highly evolved.

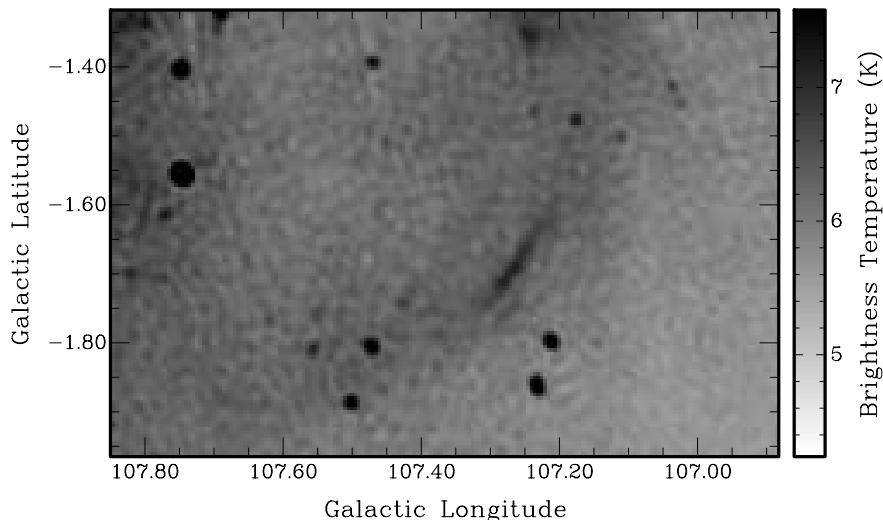


Figure 6: The SNR G107.5-1.5 (shown here in Stokes I at 1420 MHz from the CGPS Phase 1 survey) was discovered because of the intense polarized emission associated with a portion of the SNR shell around $l = 107.2$ deg, $b = -1.7$ deg. The full Stokes capability of GALFACTS can be utilized in a similar way.

2.3.2 Thermal/non-thermal separation and Spectral Analysis

Analysis of the variation of intensity as a function of frequency within the 300-MHz ALFA band and comparison with the existing Effelsberg Galactic plane surveys at both 2.7 and 5.0 GHz (for which the Arecibo resolution is well matched), will enable the determination of spectral index for both individual objects and diffuse emission from the Galactic plane. Such data should allow us to perform thermal-nonthermal separation on angular scales of a few arcminutes. Such a separation will allow the study of energy injection and energy losses of relativistic particles in the ISM associated with SNR, and the mechanism of vertical transport and diffusion of energy from the disk of the Galaxy to the halo and intergalactic space.

The Arecibo resolution at 21 cm is also comparable to the resolution of the large scale IRAS maps which have recently been reprocessed to form the IRIS data set ($\sim 4'$). IRIS images have a better intensity calibration and image quality than the original ISSA plates (Miville-Deschenes & Lagache 2005). In the context of GALFACTS such infrared images will be very useful as a means to make a thermal/non-thermal determination for individual objects. Thermal emitters such as HII regions have a much higher IR:radio brightness ratio than non-thermal emitters such as SNRs.

There exists extensive experience in the GALFACTS science team in the analysis and determination of spectral indices of both isolated sources and extended emission gained through the analysis of data obtained in the interferometer based surveys. A large suite of software tools have been developed that can easily be adapted to the analysis of GALFACTS images in this context.

2.3.3 Galactic Loops

Even the earliest radio continuum sky surveys revealed a number of “spurs” of emission seen curving away to high latitudes from the intense radiation concentrated along the Milky Way. Three of these features were soon demonstrated to trace extensive segments of small circles in the sky. This, plus their sharp outer edges, less steep inner gradients, and significant inner ridging, led to suggestions that they represent emission from old, nearby supernova remnants.

The brightest of these features is Loop I (the North Polar Spur), which is also associated with HI and X-ray emission, but is optically dark. It has an angular diameter of $\sim 115^\circ$, and lies entirely in the northern galactic hemisphere. Loop II (the Cetus Arc) is $\sim 90^\circ$ in size and a feature of the southern galactic sky, while Loop III subtends 65° and can be traced across the galactic plane. The smaller Loop IV (40° in size) lies within Loop I, although its connection, if any, to the larger feature is not clear. A number of other, weaker loops and spurs have also been identified. The major loops all have steep non-thermal continuum spectra at cm-wavelengths, and the percentage polarization of their radiation can be very high, reaching some 70% at 1.4 GHz for the high-latitude segment of Loop I. It has been suggested that their Faraday rotation displays “rotation without depolarization”, suggesting that the rotation is predominantly from a smooth, nearby foreground screen. The magnetic field of Loop I runs essentially parallel to the continuum emission ridge for $b > 45^\circ$, while the situation is more complicated below this latitude, as is the distribution of total intensity. The internal ridges of Loop I are also believed to be highly polarized.

While the proposal that the Loops represent the emission from old, nearby SNRs is the widely accepted explanation of their natures, other theories have been put forward. These include that the spurs are radio tracers of a helical component to the galactic magnetic field, that they are bubbles caused by the instability of the galactic magnetic field to cosmic ray pressure, and that Loop I is associated with the formation of the 3-kpc expanding arm via an explosion or starburst at the Galactic centre.

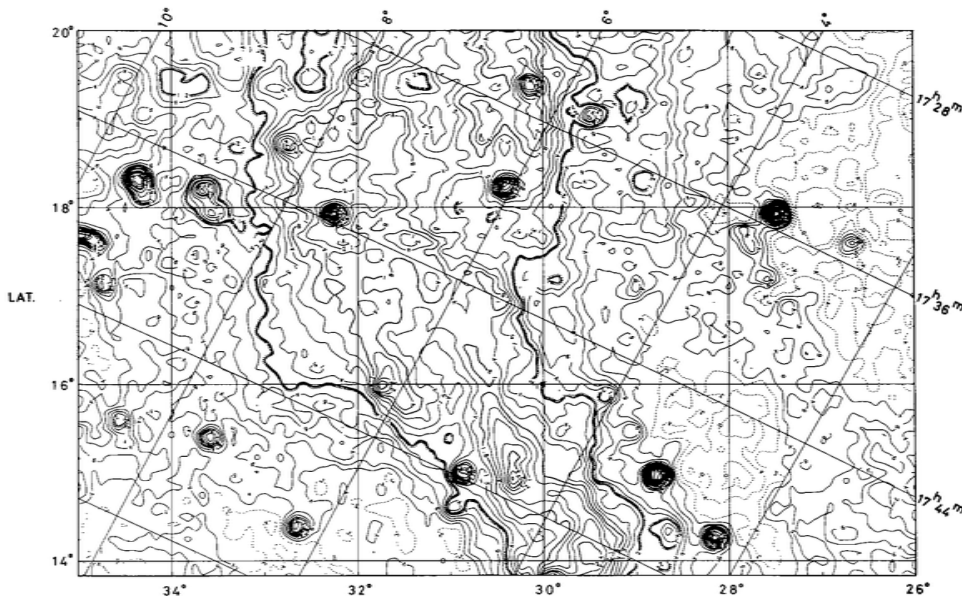


Figure 7: Contour map of the intermediate latitude total-intensity emission from the North Polar Spur at 1.4 GHz made with the Effelsberg telescope (Sofue & Reich 1979). The image is in Galactic coordinates, and the HPBW ~ 10 arcmin.

In terms of GALFACTS, the North Polar Spur section of Loop 1 runs along more than 6 hr of RA within the Arecibo sky. There is also coverage of a considerable amount of the internal ridging of Loop I, and of a large segment of Loop IV. Measurements with about 10-arcmin resolution of Loop I have shown that this object contains rich small-scale structure, both on its main arc and in internal ridging (Figure 7). The total-intensity imaging from GALFACTS would have over an order of magnitude

smaller beam area than any previously available observations of the object. Further, this would be the first polarization imaging of any of the Loops with a resolution much better than 1° . In particular, it is expected that the high polarized intensity of Loop I will allow us to trace the feature into the Galactic plane, where its total intensity emission is lost against the high confusion from the Galactic disk. In addition, the higher longitude section of Loop II will also be mapped for the first time with resolution much superior to 1 degree, as will be the case for a number of the other weaker loops and spurs.

2.4 Synergy with the *Planck* mission

2.4.1 Overview

Today’s frontier in the study of the Cosmic Microwave Background is the measurement of polarization. The initial detections by DASI and *WMAP* provided a crucial consistency check of the current ‘concordance’ cosmological model. The next generation of CMB experiments, especially the *Planck* spacecraft, aim to make precision polarization measurements which will provide the first experimental constraints on the physical mechanism of inflation, as well as giving us more precise measurements of the traditional cosmological parameters. But such measurements require accurate modelling of the polarized foreground emission, which is brighter than the most interesting (‘B-mode’) component of CMB polarization.

Partly, *Planck* will deal with this by measuring polarization in seven bands between 30 and 353 GHz, and separating CMB from foregrounds via their different spectra. However, only the lowest two *Planck* bands will be dominated by synchrotron emission, and measurements of the synchrotron polarization at lower frequencies is likely to be needed to fix an accurate spectral model at each pixel. *Planck*’s highest-frequency polarized bands will be dominated by thermal dust emission.

Together GALFACTS and *Planck* will provide not only more reliable cosmology but also a wholly new insight into the structure of the Galaxy’s magnetic field, from comparison of synchrotron and dust polarization.

2.4.2 Physics of CMB polarization

In the last 25 years, essentially *all* direct evidence for new fundamental physics has come from astrophysical and cosmological data. Specifically, the particle physics Standard Model has been extended to include non-zero neutrino masses and neutrino flavour mixing thanks to solar neutrino observations, while no less than three new sectors of physics entirely outside the Standard Model have been revealed by cosmology: non-baryonic matter, dark energy, and inflation. Of these, the least well characterized is inflation: while CMB observations are impressively in accord with generic inflationary predictions, the physics of the inflation field is essentially unknown. The deep excitement driving CMB polarization work is that it can measure or at least limit from above the energy scale of inflation, currently uncertain by fourteen orders of magnitude — between the limit from current results ($\sim 1.5 \times 10^{16}$ GeV) and the electro-weak scale (100 GeV). Fortunately, the most plausible value is the GUT scale (10^{15} – 10^{16} GeV) which is potentially within experimental reach. The value of this energy is obviously a major clue to the physics, and many proposed models will be excluded when it is known.

Because the transition to an optically thin universe at the ‘epoch of last scattering’ took a finite time ($\Delta z \approx 80$), Thomson scattering on the ‘photosphere’ of the early universe produces polarization associated with intensity anisotropies. Averaging through the last scattering zone, we expect (e.g. Hu & White 1997) so-called ‘E-mode’ polarization of a few percent of the fluctuation level (itself a few parts in 10^5), and this has been detected (Kovac *et al.* 2002, Kogut *et al.* 2003, Readhead *et al.* 2004, Leitch *et al.* 2005). This CMB polarization is a straightforward prediction from the standard theory and provides an important cross-check on cosmological deductions from the total intensity fluctuations. In the future, accurate measurement of the E-mode polarization will give increased precision for the derived cosmological parameters.

Modifications of the basic CMB polarization provide two more fundamental cosmological diagnostics.

First, the large-scale CMB fluctuations detected by COBE could be caused by fluctuations in the scalar gravitational potential (in effect, matter inhomogeneities) or by tensor fluctuations (gravitational waves). Gravitational waves would distort the polarization pattern, producing ‘B-mode’ fluctuations (orthogonal to the E-modes) which are otherwise strictly zero. The scalar-to-tensor, or E/B amplitude ratio is proportional to the square of the inflationary energy scale in most models, giving us our route to inflation physics. This signature would be predominantly on scales larger than the horizon at CMB emission ($\approx 0.5^\circ$).

Second, due to re-ionization of the intergalactic medium, the CMB fluctuations are seen through a mist with a significant optical depth to scattering. Naturally, this scattering is associated with a polarization signal, strongest on the horizon scale at the epoch of re-ionization. The most surprising result from *WMAP* was the claimed detection of a very strong re-ionization signal, implying re-ionization at $z \geq 20$. This will be independently checked by *Planck*. By definition this horizon is larger than that at the (earlier) CMB emission surface.

Both these key diagnostics involve very large-scale (several degrees) structure in the CMB polarization, so can only be accurately measured with all-sky surveys. Both signatures are expected to be very weak, with amplitudes below $1 \mu\text{K}$.

2.4.3 Contribution of GALFACTS to foreground subtraction

The high-frequency spectrum of Galactic synchrotron emission is not well known. Steepening above ~ 10 GHz is expected given the knee in the cosmic ray electron energy spectrum at a few GeV (e.g. Boezio *et al.* 2000). We expect both knee frequency and initial spectral index to vary with position in the Galaxy, giving three spectral parameters to be fixed even for emission from a homogeneous region. Hence accurate modelling requires data at synchrotron-dominated frequencies well below the *Planck* bands.

Existing low-frequency data (e.g. 21 cm) is strongly affected by Faraday rotation and depolarization, so that the polarized emission cannot be extrapolated directly to high frequency. ALFA will largely overcome this defect by recovering the Rotation Measure from within its 300 MHz bandwidth, while the high resolution will minimize beam depolarization. Further, much of the GALFACTS region is at high latitude, the target zone for CMB measurements and a region where line-of-sight depolarization is expected to be minimal. Finally, GALFACTS covers the dominant synchrotron feature in the high-latitude sky, the North Polar Spur.

2.4.4 Contribution of *Planck* to Galactic science

Study of the Galaxy is a major secondary objective of *Planck*. The *Planck* data itself, essentially free of Faraday rotation ($\lambda \leq 1$ cm) will tie down the projected direction of the magnetic field via both synchrotron and dust emission, wherever foregrounds dominate. In the highest-frequency bands, this is likely to extend far away from the plane.

To zeroth order, excluding features such as SNR, cosmic rays are believed to be spread rather smoothly through the ISM, so the synchrotron emissivity is mainly modulated by the field strength. In contrast, dust is associated only with the colder ISM components. Since dust alignment is believed to be saturated, the dust polarized emissivity depends mainly on the dust density and not at all on the field strength. Hence comparison of GALFACTS synchrotron and *Planck* dust polarization maps will yield new insights into the coherence of the magnetic field between different regions. This is especially true because the two dust-dominated *Planck* bands, 217 and 353 GHz, have a resolution of 5 arcmin, much better matched to ALFA than to the ~ 30 arcmin resolution of the *Planck* synchrotron-dominated bands (30 & 44 GHz).

2.5 Compact Sources

Covering the declination range, $-0.8^\circ < \delta < 37.8^\circ$, GALFACTS will span a sky area of ~ 4.0 sr with a theoretical rms noise in images of combined polarizations, of about $60 \mu\text{Jy}/\text{beam}$ on cold sky. For Stokes-I this is well below the rms confusion level due to the point source background of ~ 2 mJy/beam.

Standard 1.4-GHz source counts (e.g. Condon 1984) lead us to expect that $\sim 230,000$ discrete extragalactic sources with flux densities greater than 10 mJy/beam will be detected by GALFACTS. At this flux density level, the extragalactic source population will still be dominated by powerful AGNs. However, about a quarter of the sources are expected to be normal and starburst galaxies, low luminosity AGNs (such as LINERs), and Seyfert galaxies. Most of these will have been detected earlier by NVSS, although GALFACTS, with its $3'$ beam, will be more sensitive to low surface brightness features. Hence, we hope to detect extended halos of nearby galaxies and clusters of galaxies, as well as identify a number of giant radio sources (size $\gtrsim 1\text{Mpc}$) that could have been considered to be a pair of unconnected sources in NVSS.

2.5.1 Polarization properties of Compact Sources

The confusion level in linear polarization will be well below the total intensity value (in fact about two orders of magnitude less, $\sim 20 \mu\text{Jy}/\text{beam}$). Hence, we can make a very sensitive, unconfused survey of the polarization properties of radio sources. The resultant catalogue of polarized sources will have two important applications. First, these data will allow us to produce a “log $N - \log L$ ” distribution for polarization from extragalactic radio sources down to polarized fluxes as low as 0.4 mJy. Such a distribution has never been calculated at these levels (cf. Mesa *et al.*, 2002; Tucci *et al.*, 2004), but can prove vital for characterizing the point source contribution to polarized CMB experiments, and for providing an observational underpinning for the “rotation measure grid” that will be seen by the Square Kilometre Array (Gaensler *et al.* 2004). Second, there are hints at much higher flux levels that the fractional polarization gets larger for increasingly fainter radio sources Mesa *et al.* (2002). This is not understood, but may be indicative of a slightly different population emerging at lower flux levels. The much deeper data-set to be obtained here will be able to resolve this issue.

For unresolved sources, polarization variability is expected to be detected on both sub-monthly and 10 year time scales, the extremely active Blazar (BL Lac and quasar) population being known to show both percentage polarization and position-angle variations on such time scales. GALFACTS will enhance the number of individual sources known to show such characteristics, and allow detailed, unbiased statistical studies of this phenomenon.

The sensitivity of Arecibo, combined with the multiple channels across the 300-MHz bandwidth of ALFA, would permit a complete rotation measure (RM) survey of sources with detected linear polarization. To emphasize the power of having available a 300-MHz bandwidth for polarization measurements, the change of position angle across the band is $\Delta\theta = 1.22 \times \text{RM}$ degrees, (or one full 180° turn for an RM of ~ 150 rad/m²).

2.5.2 Exotic Objects: Variability and Circular Polarization

With the planned observing strategy, each point in the sky will be visited twice, with the interval between visits being distributed between 1 and 28 days, (see Section 3.1). Given the large number of (extragalactic) sources that will be measured, extremely interesting statistics on the short-term variability properties of all sources will be obtained. We note that the full sensitivity of the observations can be usefully employed to study variability, as the effects of confusion will be essentially identical at the two epochs. Thus we anticipate being able to search for variable and transient sources at the level of about 0.4 mJy/beam ($\sqrt{2} \times 5 \times \sigma_{\text{noise}}$ for a single transit), i.e. well below the r.m.s. confusion limit. In addition, comparison with the accurate flux densities of NVSS will provide variability information on a time scale of 10 yr. The sky has never before been searched systematically for variations to this depth, and over such a large area.

We will also search the Stokes-V channel for evidence of highly circularly polarized (CP) sources, such as pulsars and flares stars. Serendipitous detection of unexpectedly circularly polarized sources would also be a first. There has been a recent surge of interest in CP observations with detections of $0.5 > V > 0.1\%$ of CP in AGNs and galactic microquasars using ATCA and the VLA (Rayner *et al.* 2000; Bower *et al.* 2002; Fender *et al.* 2000). All of these have been targeted observations. On the theoretical front, Kennett and Melrose (1998) claimed that significant circular polarization can originate due to propagation of synchrotron radiation through relativistic plasma. GALFACTS will provide the data for a sensitive unbiased search for circularly polarized sources. The Stokes-V detection limit for GALFACTS is not yet known, as it depends upon calibration issues that are presently under investigation using the ALFA precursor observations. However, we have easily achieved Stokes V to residual levels of 0.1% in very preliminary calibration (see Fig. 12). Further improvements are expected as we refine the calibration.

3 Observations and Data Processing

3.1 Observations

Because of the logistics of observing, GALFACTS will be separated into three survey regions; a south survey consisting of the portion of the sky south of zenith angle 1.5° on the southern meridian, ($-0.8^\circ < \delta < 17.2^\circ$), a north survey of the sky north of zenith angle 1.5° on the northern meridian ($19.8^\circ < \delta < 37.8^\circ$), and a zenith survey of the strip within $Za < 2.0^\circ$, ($16.3^\circ < \delta < 20.3^\circ$), together providing complete coverage of the 12,734 square degrees of sky from ($-0.8^\circ < \delta < 37.8^\circ$)

The observations for the south and north surveys will be carried out in the manner developed during the precursor observations. ALFA is rotated to 0° and driven up and down the meridian at a rate of 1.53 degrees/sidereal minute. The geometry is illustrated in Figure 8. This geometry produces parallel tracks on the sky from each of the ALFA beams with a RA scan separation of $1.83'$. For scans that are 18° long in declination, 28 scan patterns are required to fully sample the survey in Right Ascension, i.e. 28 separate observing runs. The north and south surveys thus each require 672 hours of observations (28×24 hours), or a total of 1344 hours.

The missing strip at $Za < 1.5^\circ$, will be filled in with “azimuth-wags”, with the telescope fixed at $Za = 10^\circ$. The wags will be centred on an azimuth close to 90° . The scanning speed in azimuth will be 8.6 deg/min ($1.5/\sin 10^\circ$), producing a separation of the beams equal to $1.83'$. The scan pattern on the sky will thus be the same as for the north and south surveys except that ALFA will be rotated by 90° . The azimuth scans will be 23° long, yielding a zenith angle span of 4° through the zenith. These scans will overlap the north and south surveys by 0.5 degrees, allowing seamless merging of the images from the three regions. Each pair of back and forth azimuth wags will take 6 minutes (2.7 minutes per scan plus turn-around time). A fully sampled survey takes 7 different wag sets. Therefore to cover 24 hours of Right Ascension will take 168 hours (7×24 hours).

The complete GALFACTS survey will thus require a total of 1512 hours of observations. The influence of the Sun in the polarized far side-lobes makes it impossible to secure reliable polarimetry during the day. GALFACTS must be observed at night. Our optimal time allocation would be one observing session per quarter of three hours per night for 28 consecutive nights. Each observing session would provide fully sampled data for a $15^\circ \times 18^\circ$ region. The time allotment would be 336 hours year year for four years, after which time observations for the north and south surveys would be complete. GALFACTS observations would be completed in year five by carrying out the zenith survey.

With these observing parameters on average each point (beam area) on the sky has an effective integration time (dwell time within one FWHM of the beam) of 7.8 seconds. We will use the new P-ALFA/Continuum spectrometer to make spectro-polarimetric cubes, (intensity as a function of α, δ, ν), in each of I, Q, U and V, with 1024 spectral channels over a 300 MHz bandwidth. Assuming an effective bandwidth of 250 MHz (to account for roll off and loss to RFI), and an average SEFD of 3.5 Jy, the theoretical 1σ noise level integrated over the full band in Stokes I is $\sim 60 \mu Jy$, (about $85 \mu Jy$ per

is carried out separately for each frequency channel. Initial Stokes image cubes are created by gridding the basket-weaved, time-series spectra.

5. Incorporate Very Low Spatial Frequencies

We will use the northern-sky ($-35^\circ < \delta < 90^\circ$), DRAO 26-m, polarization survey (Wolleben *et al.* 2005) to establish polarization zero-levels. The DRAO survey covers the entire GALFACTS area with a beamwidth of $36'$, and well calibrated absolute zero levels in Q and U. Techniques and software for integrating low-spatial frequencies into images have been developed at DRAO. We will adapt this software for our images. Stokes I zero levels will be linked to the Effelsberg surveys.

6. Multi-beam Clean

This step will be applied to the Stokes I image to remove the near-in sidelobes. Accurate point source response functions (beam maps) have been secured from calibration observations. We have developed an algorithm for cleaning the images constructed from the the seven ALFA beams, and will implementing it as the next phase in our software development. One of the outputs of this stage is a clean component representation of the Stokes I map which will be used for the next step.

7. Remove Stokes-I Leakage polarization side-lobe Patterns

The clean component representation of the Stokes I map will be convolved with the Stokes near-in sidelobe patterns (residual to step 3). This pattern is zero at beam centre after step 3, but the classical “butterfly” pattern remains. The convolved “leakage” images will be subtracted from the polarization images to remove this effect.

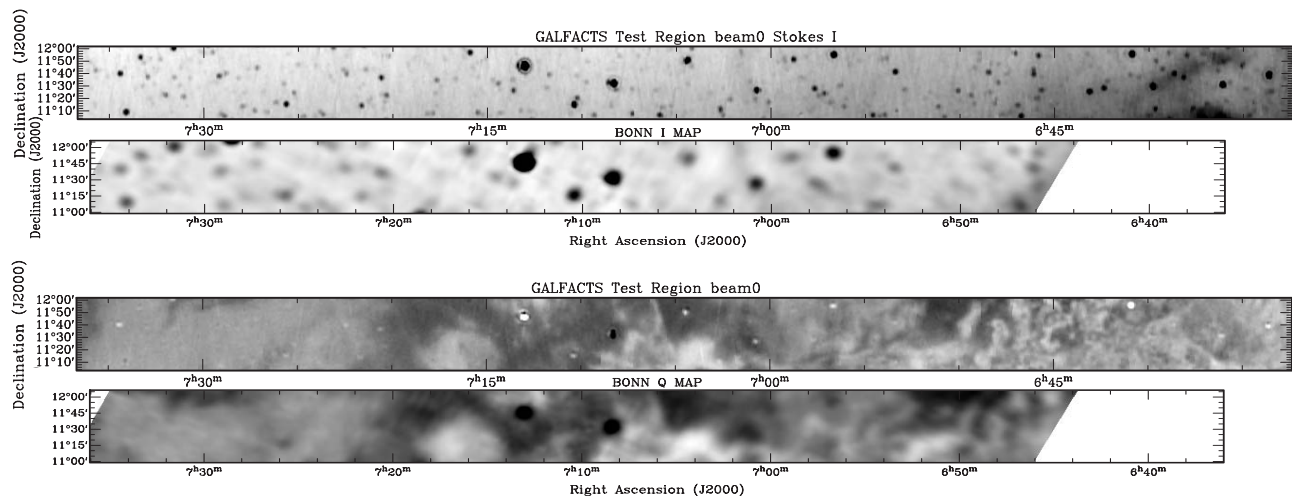


Figure 10: Images of the GALFACTS test region in Stokes I (top pair of images) and Stokes U (bottom pair). The image from the GALFACTS precursor observations (resolution $3.5'$) is the top image in each pair and the Effelsberg image (resolution $10'$) is at bottom. The Galactic Plane is toward the right in these images where a Stokes-I filament is seen and possibly associated turbulent-like Faraday rotation structure.

After step 7, the final Stokes image products will be created, as described in the next section. From the Stokes images we will extract images of the RM of the diffuse polarized radiation from the Galaxy as well as a catalogue of compact sources including RM's. Software for this purpose that has been developed at the University of Calgary for the CGPS (Brown *et al.* 2003), will be adapted for GALFACTS.

Software development has been completed to step 4. Band averaged images of the GALFACTS pilot region from the precursor observations are shown in Figure 10. The precursor observations imaged a

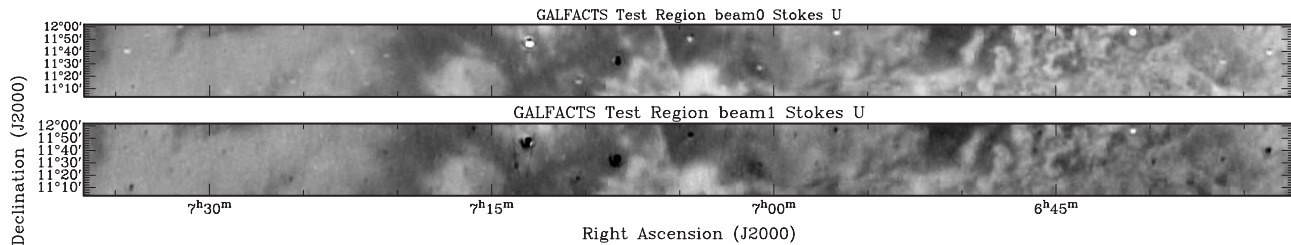


Figure 11: Comparison of GALFACTS precursor ALFA Stokes-U maps with data taken from the central ALFA beam (top) and an outer beam (bottom). The diffuse polarised emission is reproduced by both beams. The Stokes-I leakage response is different for the two beams, yielding a systematic difference in the response to point sources. This effect at beam centre is removed using observations of unpolarised sources.

$10^\circ \times 1^\circ$ ($\alpha \times \delta$) region in fast meridian scanning mode. Data were taken in 256 spectral channels over a 100 MHz bandwidth. Since we wished to test our ability to construct full Stokes images, the test region was chosen to overlap one of the areas mapped as part of the Effelsberg mid-latitude polarization survey (Uyaniker *et al.* 1999). Figure 10 shows Stokes I and U images for both the GALFACTS test observations and the Effelsberg survey. The GALFACTS test images are constructed by averaging channels over about 80 MHz. Comparison of the Arecibo and Effelsberg images shows the clear advantage of the higher resolution and sensitivity of Arecibo. The Arecibo Stokes I image goes much deeper (the faintest source discernible has a flux density of about 4 mJy). The Stokes-U Arecibo image reproduces the structures seen at Effelsberg while showing much more detail.

The Arecibo U image has not yet been corrected for Stokes-I leakage terms. This has little effect on the diffuse emission, since these structures are a product of the Faraday Screen and have no Stokes-I counterpart. This is demonstrated in Figure 11, where we show Stokes-U images constructed from the central ALFA beam (beam 0) and one of the outside beams. The diffuse emission is virtually identical in the two images. Instrumental U is apparent for many of the stronger “point” sources in the I map and differs for the two ALFA beams. The effect of this leakage at beam-centre is well removed with the beam-centre Mueller matrix corrections derived from observations of unpolarized sources. Figure 12 shows the beam-centre spectral response for a polarized point source in the test region after applying a preliminary frequency-dependent correction. The source has 15% linear polarization, $V < 0.1\%$. In agreement with the values derived from Effelsberg data. The variation of polarization angle with wavelength across the 80 MHz band allows us to derive a Rotation Measure of $+34 \text{ rad/m}^2$. The RM of this source has not been measured previously.

3.3 Data Management and Archiving

As described in the previous section, the stage-1 processing at the Arecibo Observatory, time averages the 1 ms sampled data to 0.2-s samples. This time series of auto- and cross-correlated spectra with cal signal off and cal signal on are the raw data that will be archived. An original copy of these data will be archived at Arecibo, and a copy will be sent to (by removable disk pack) to the University of Calgary radio astronomy laboratory for processing into images. Once the copy of the data at Calgary is validated, the 1ms data set from which it is derived will be deleted. The data rate out of stage 1 is a modest value of 0.9 Gigabytes per hour. The archive of 0.2-s raw data for the entire GALFACTS project will occupy about 1.5 Terabytes.

The GALFACTS image data will be of similar size, totalling about 150 Megabytes per square degree. The GALFACTS survey of 12,734 square degrees will thus take up about 1.9 Terabytes. The data products for distribution to the public domain will be image sets of 5×5 degree. Each image set will consist of spectral cubes in each of Stokes I , Q , U , V , as well as the band-averaged images and HI column images from integration over the HI channels. Each image set will be about 3.8 Gigabytes in size (a convenient size for storage on a single DVD). The complete GALFACTS data will consist of

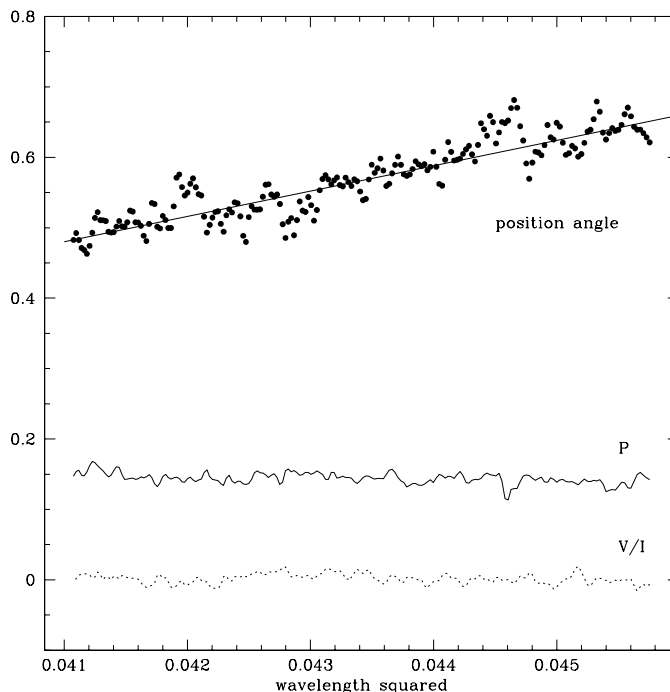


Figure 12: Preliminary spectro-polarimetry of a polarized source in the test region ($\alpha = 07\ 08\ 17$, $\delta = 11\ 32\ 55$). An initial estimate of the frequency-dependent, beam-centre Stokes I leakage terms has been applied. The plot shows polarization position angle (points) across the 80 MHz band of the precursor observations, and the fractional linear and circular polarization. The source is about 15% linearly polarized and the fit (solid line) to polarization position angle with wavelength squared yields a RM of $34\ \text{rad m}^{-2}$. This value is similar to the RM of two sources in this general direction (+7 and +90) from the RM catalogue of Broten *et al.* (1988). The average value of circular polarization is 0.1%.

about 400 of these image sets.

The 0.2-s sampled raw data, and the GALFACTS image products, will be archived at the University of Calgary, Radio Astronomy Laboratory. The image data will also be archived for access by the public domain and will be integration into the Virtual Observatory, by the Canadian Astronomy Data Centre (CADC) at the Herzberg Institute of Astrophysics. The CADC and HIA are part of the National Research Council of Canada.

Image data products will be made publicly available as soon as they are completely processed and their quality assessed. Quality assessment will be carried out by the project data processing team and the expert data users in the Consortium. Preliminary release of data at interim stages to the GALFACTS consortium will be made available through a project web site and ftp site at the University of Calgary.

3.4 Project Organization

The GALFA continuum sub-consortium submitting this proposal consists of 20 researchers, many of whom have substantial experience in survey projects of this scope and also expertise in technical issues and scientific interpretation of polarimetric observations. It is anticipated that among the University members of the group, 5-6 additional graduate students will join the project in 2006.

We will form an observing team that will be responsible for carrying out the observations at Arecibo. As noted in section 3.2, pipeline processing of the data will be carried out at Arecibo and the University of Calgary, where a software engineer, Jeff Dever, has been hired for this purpose. The data products will be distributed in preliminary form to the consortium as soon as possible to facilitate early science.

Conversion of the images to Healpix format for use with WMAP and eventually Planck will be done at the University of Manchester.

The scientific goals of the project are diverse covering the role of magnetic fields in a range astrophysical contexts. Many of the scientific projects outlined in this proposal will be executed by collaborative teams among the consortium. We plan to hold annual science meetings for the project to present and exchange ideas, report progress, and develop plans. We will also submit annual project reports to the NAIC. With the proposed observing schedule, over the course of the first year we will have observed close to 20% of the survey, with data covering a range of Galactic latitude. Polarization structure from the Faraday screen are ubiquitous. We expect substantial early science will be reported at the first project science meeting.

3.5 Commensal Observations

HI Survey of the Arecibo Sky

A GALFA-HI consortium team propose to carry out a high-resolution survey of HI emission from the Arecibo sky by taking data with the GALFA-HI spectrometer while GALFACTS is observing with the P-ALFA/Continuum spectrometer. The commensal GALFA-HI survey proposal is being submitted separately.

Commensal OH observations with the WAPP Backend

With the possibility of using multiple backends with ALFA, a team is planning a proposal to use the WAPPs with the 50 MHz bandwidth per beam, two polarization, and 8192 spectral channels, to conduct a commensal blind OH 18 cm maser survey. The spectral resolution after Hanning smoothing is 6.1 kHz (1.1 km/s), and the expected rms noise level per spectral channel is ~ 19 mJy/beam. The proposed WAPPs configuration would result in adequate spectral resolution to detect narrow OH maser emission lines in the Galaxy, while at the same time searching for low z extragalactic sources, complimenting the ALFALFA survey that targets OH megamaser emission in the range $0.16 < z < 0.25$. A commensal proposal will be submitted for a later deadline.

References

- Achterberg, A., Blandford, R. D., & Reynolds, S. P. 1994, *A&A*, 281, 220
- Armstrong, J. W., Rickett, B. J., & Spangler, S. R. 1995, *ApJ*, 443, 209
- Basu, S., Johnstone, D., & Martin, P. G. 1999, *ApJ*, 516, 843
- Beck, R. 2004, *Ap&Ss*, 289, 293
- Beck, R. *et al.* 1996, *ARA&A*, 34, 155.
- Beck, R. 2000, *Philos. Trans. Roy. Soc. London A*, 358, 777
- . 2001, *Space Science Reviews*, 99, 243
- Beck, R., Brandenburg, A., Moss, D., Shukurov, A., & Sokoloff, D. 1996, *ARA&A*, 34, 155
- Beck, R. & Gaensler, B. M. 2004, *New Astronomy Reviews*, 48, 1289
- Berkhuijsen, E.M., Haslam, C.G.T., Salter, C.J., 1971, *A&A*, 14, 252
- Beuermann, K., Kanbach, G., & Berkhuijsen, E. M. 1985, *A&A*, 153, 17
- Boezio, M., *et al.* 2000. *ApJ*, 532, 653.

- Bower, G.C., Falcke, H, Mellon, R.R., 2002, ApJL, 578, L103
- Brentjens, M. A. & de Bruyn, A. G. 2004, in "Proceedings of The Riddle of Cooling Flows in Galaxies and Clusters of Galaxies", <http://www.astro.virginia.edu/coolflow/proc.php>
- Brogan, C. L., Frail, D. A., Goss, W. M., & Troland, T. H. 2000, ApJ, 537, 875
- Broten, N. W., MacLeod, J. M. and Valeé, J. P. 1988, A&SS, 141, 303
- Brown, J. C., Taylor, A. R., Jackel, J. B. 2003, ApJS, 145, 213
- Brown, J. C. & Taylor, A. R. 2001, ApJ, 563, L31
- Chevalier, R. A. 1999, ApJ, 511, 798
- Condon, J. 1984, ApJ, 287, 461
- Dennison, B., Simonetti, J. H., & Topasna, G. A. 1999, BAAS, 195, 53.09
- Elmegreen, B. G., & Scalo, J. 2004, ARA&A, 42, 211
- Fender, R., Rayner, D., Norris, R., Sault, R.J., Pooley, G., 2000, ApJ, 530, L29
- Ferrière, K. M. 2001, RvMP, 73, 1031
- Fürst, E. & Reich, W. 2004, in The Magnetized Interstellar Medium, ed. B. Uyaniker, W. Reich, & R. Wielebinski (Katlenburg-Lindau: Copernicus GmbH), 141–146
- Gaensler, B. M., Dickey, J. M., McClure-Griffiths, N. M., Green, A. J., Wieringa, M. H., & Haynes, R. F. 2001, ApJ, 549, 959
- Gaensler, B. M. & Wallace, B. J. 2003, ApJ, 594, 326
- Gaensler, B. M., Beck, R., & Feretti, L. 2004, New Astronomy Reviews, 48, 1003
- Gaustad, J. E., McCullough, P. R., Rosing, W., & Van Buren, D. 2001, PASP, 113, 1326
- Gray, A. D., Landecker, T. L., Dewdney, P. E., & Taylor, A. R. 1998, Nature, 393, 660
- Goldreich, P., & Sridhar, S. 1997, ApJ, 485, 680
- Goldreich, P., & Sridhar, S. 1995, ApJ, 438, 763
- Han, J. L., Manchester, R. N., Berkhuijsen, E. M., & Beck, R. 1997, A&A, 322, 98
- Han, J. L., Manchester, R. N., Lyne, A. G., & Qiao, G. J. 2002, ApJ, 570, L17
- Han, J. L. & Qiao, G. J. 1994, A&A, 288, 759
- Han, J.-L. & Wielebinski, R. 2002, Chin. J. Astron. Astrophys., 2, 293
- Haslam, C. G. T., Quigley, M. J. S., Salter, C. J., MNRAS, 147, 405
- Haverkorn, M., Gaensler, B. M., McClure-Griffiths, N. M., Dickey, J. M., & Green, A. J. 2004, ApJ, 609, 776
- Haverkorn, M., Gaensler, B. M., McClure-Griffiths, N. M., Dickey, J. M., & Green, A. J. 2005, submitted to ApJ
- Haverkorn, M., Katgert, P., de Bruyn, A. G. 2003a, A&A, 403, 1045

- Haverkorn, M., Katgert, P., & de Bruyn, A. G. 2003b, *A&A*, 404, 233
- Heiles, C., Goodman, A.A., McKee, C.F. & Zweibel, E.G. 1993, in *Protostars and Planets III*, eds E. H. Levy & J. I. Lunine, University of Arizona Press, p. 279
- Heiles, C., Chu, Y.-H., & Troland, T. H. 1981, *ApJ*, 247, L77
- Hu, W., White, M. 1997. *New Astr.* 2, 323
- Indrani, C. & Deshpande, A. A. 1998, *New Astronomy*, 4, 33
- Jun, B.-I. & Norman, M. L. 1996a, *ApJ*, 465, 800
- . 1996b, *ApJ*, 472, 245
- Kennett, M., Melrose, D. B., 1998, *Publ. Astron. Soc. Aust.*, 15, 211
- Kogut, A. et al. 2003. *ApJS*, 148, 161.
- Kothes, R., Landecker, T. L., & Wolleben, M. 2004, *ApJ*, 607, 855
- Kothes, R. 2003, *A&A*, 408, 187
- Kothes, R., Landecker, T. L., Foster, T., & Leahy, D. A. 2001, *A&A*, 376, 641
- Kovac, J. M. *et al.* 2002. *Nature*, 420, 772
- Kulsrud, R. M. 1999, *ARA&A*, 37, 37
- Leitch, E. M., *et al.* 2005. *ApJ*, 624, 10
- Matthews, B.C., Fiege, J.D. & Moriarty-Schieven, G. 2002, *ApJ*, 569, 304.
- Matsui, Y., Long, K. S., Dickel, J. R., & Greisen, E. W. 1984, *ApJ*, 287, 295
- Mesa, D., Baccigalupi, C., De Zotti, G., Gregorini, L., Mack, K.-H., Vigotti, M., & Klein, U. 2002, *A&A*, 396, 463
- Milne, D. K. 1990, in *IAU Symposium 140: Galactic and intergalactic magnetic fields*, ed. R. Beck, P. P. Kronberg, & R. Wielebinski (Dordrecht: Kluwer), 67–62
- Minter, A. H., & Balsaer, D. 1997, *ApJ*, 484, L133
- Minter, A. H., & Spangler, S. R. 1997, *ApJ*, 485, 182
- Minter, A. H., & Spangler, S. R. 1996, *ApJ*, 458, 194
- Miville-Deschnes, M.-A. & Lagache, G. 2005, *ApJSS*, 157, 302
- Miville-Deschênes, M.-A., Joncas, G., & Durand, D. 1995, *ApJ*, 454, 316
- Normandeau, M., Taylor, A. R., & Dewdney, P. E. 1996, *Nature*, 380, 687
- Ostrowski, M. 1999, *A&A*, 345, 256
- Ramkumar, P. S., & Deshpande, A. A. 1999, *J. Astrophys. Astr.*, 20, 37
- Rand, R. J. & Lyne, A. G. 1994, *MNRAS*, 268, 497
- Rayner, D., Norris, R., Sault, R.J., 2000, *MNRAS*, 319, 484

- Readhead, A. C. S. *et al.* 2004. *Science*, 306, 836
- Reich *et al.* (2001), *A&AS*, 376, 861
- Rickett, B. J., & Coles, Wm. A. 2005, American Astronomical Society Meeting 205, #111.10
- Simonetti, J. M. 1992, *ApJ*, 386, 170
- Sofue, Y. *et al.* 1986, *ARA&A*, 24, 459.
- Sofue Y. & Reich, W., 1979, *A&AS*, 38, 251
- Shukurov, A. & Berkhuijsen, E. M. 2002, *MNRAS*, 342, 496
- Sokoloff, D. D., Bykov, A. A., Shukurov, A., Berkhuijsen, E. M., Beck, R., & Poezd, A. D. 1998, *MNRAS*, 299, 189
- Taylor, A.R. *et al.* 2003, *AJ*, 125, 3145.
- Terebey, S., Fich, M., Taylor, R., Cao, Y., & Hancock, T. 2003, *ApJ*, 590, 906
- Tribble, P. C. 1991, *MNRAS*, 250, 726
- Troland, T. H. & Heiles, C. 1986, *ApJ*, 301, 339
- Tucci, M., Martínez-González, E., Toffolatti, L., González-Nuevo, J., & De Zotti, G. 2004, *MNRAS*, 349, 1267
- Tucci, M., Carretti, E., Cecchini, S., Nicastro, L., Fabbri, R., Gaensler, B. M., Dickey, J. M., & McClure-Griffiths, N. M. 2002, *ApJ*, 579, 607
- Tucci, M., Carretti, E., Cecchini, S., Fabbri, R., Orsini, M., Pierpaoli, E., 2000. *New Astr.* 5, 181
- Uyaniker, B., Landecker, T. L., Gray, A. D., & Kothes, R. 2003, *ApJ*, 585, 785
- Uyaniker, B. & Landecker, T. L. 2002, *ApJ*, 575, 225
- Uyaniker, B., Fürst, E., Reich, W., Reich, P., Wielebinski, R. 1999, *A&AS*, 138, 31
- Wolleben, M. & Reich, W. 2004, *A&A*, 427, 537
- Wolleben, M., Landecker, T. L., Reich, W, Wielebinski, R. 2005, *A&A*, in preparation.